Chaos and Correlated Avalanches in Excitatory Neural Networks with Synaptic Plasticity

Fabrizio Pittorino,[1,2] Miguel Ibáñez-Berganza,[2] Matteo di Volo,[3] Alessandro Vezzani,[4,1] and Raffaella Burioni[1,2]

[1]*Dipartimento di Scienze Matematiche, Fisiche e Informatiche, Università di Parma, via G.P. Usberti, 7/A—43124 Parma, Italy*
[2]*INFN, Gruppo Collegato di Parma, via G.P. Usberti, 7/A—43124 Parma, Italy*
[3]*Group for Neural Theory, Laboratoire de Neurosciences Cognitives, INSERM U960, École Normale Supérieure, Paris 75005, France*
[4]*IMEM-CNR, Parco Area delle Scienze, 37/A-43124 Parma, Italy*

A collective chaotic phase with power law scaling of activity events is observed in a disordered mean field network of purely excitatory leaky integrate-and-fire neurons with short-term synaptic plasticity. The dynamical phase diagram exhibits two transitions from quasisynchronous and asynchronous regimes to the nontrivial, collective, bursty regime with avalanches. In the homogeneous case without disorder, the system synchronizes and the bursty behavior is reflected into a period doubling transition to chaos for a two dimensional discrete map. Numerical simulations show that the bursty chaotic phase with avalanches exhibits a spontaneous emergence of persistent time correlations and enhanced Kolmogorov complexity. Our analysis reveals a mechanism for the generation of irregular avalanches that emerges from the combination of disorder and deterministic underlying chaotic dynamics.

Networks of spiking neurons feature a wide range of dynamical collective behaviors that are believed to be crucial for brain functioning [1]. Next to uncorrelated and asynchronous dynamics, quasisynchronous phases and regimes of irregular activity have been observed, showing a still unexplained degree of correlation that could encode part of the neural function [2–7]. Understanding the mechanisms that generate such experimentally observed collective behaviors and the transition between them is a major goal in theoretical neuroscience [1,8–15]. A particularly interesting dynamical signature of collective irregular regimes are *avalanches* or bursts of spiking neurons with heavy-tailed distributions of activity [6,16,17]. Interestingly, in cortical networks, irregular activity at the collective level [18,19] and avalanches characterized by power law distributions have been widely observed both *in vitro* and *in vivo* [20–23]. These regimes are thought to be closely related to information processing in the cortex [24–26] and to adaptive [27] and healthy [28] behavior.

Several mechanisms leading to irregular dynamics and bursts in networks of spiking neurons have been proposed. Irregular dynamical phases have been related to a balance between excitatory and inhibitory inputs [29,30] or to a disorder in the network or in the couplings [11,31] as crucial ingredients. Power law distributed avalanches have been attributed to synaptic plasticity with a stochastic noise in the charging [32–36] or to dynamical mechanisms inspired by self-organized criticality (SOC) [27,37,38]. The balance between excitation and inhibition plays an important role in the latter dynamical regime as well [39], and a relation between uncorrelated dynamics in a network of stochastic units and power law scaling has been proposed [40,41].

In this Letter we show that correlated irregular dynamics can be observed in homogeneous deterministic networks of

N identical purely excitatory spiking neurons endowed with synaptic plasticity, coupled by an all to all, mean field (MF), interaction. In this case, all neurons are synchronized but, for small enough synaptic decay time, the system displays a period doubling transition from a periodic phase to synchronous chaos [42,43]. Such a transition is determined by the competition among the system time scales in the strong and weak coupling limits. For vanishing synaptic decay time, the dynamics can be reduced to a one dimensional map.

In the presence of disorder in the couplings, we show that the dynamics exhibits three phases, depending on the interaction strength and synaptic decay time. In particular, next to the quasisynchronous and the asynchronous regimes [44], a phase characterized by power law distributed avalanches emerges in correspondence to the chaotic phase of the homogeneous MF model. Chaos is preserved in this dynamical phase, as confirmed by the computation of the Lyapunov exponents, and it is characterized by the onset of strong temporal correlations and high complexity. Our analysis uncovers a connection between dynamical stability and emergent avalanche activity in the presence of short-term synaptic plasticity, that may go beyond our particular case of study.

We consider a disordered random network of leaky integrate-and-fire (LIF) neurons [45] connected via the Tsodyks-Uziel-Markram (TUM) model for short term synaptic plasticity [46]. Within a degree based mean field approximation (DMF), for each neuron $i = 1 \ldots N$ the dynamic is defined by three differential equations:

$$\dot{v}_i(t) = a - v_i(t) + g k_i Y(t), \qquad (1)$$

$$\dot{y}_i(t) = -\frac{y_i(t)}{\tau_{\text{in}}} + u[1 - y_i(t) - z_i(t)]S_i(t), \qquad (2)$$

$$\dot{z}_i(t) = \frac{y_i(t)}{\tau_{\text{in}}} - \frac{z_i(t)}{\tau_R}, \qquad (3)$$

where $v_i(t)$ is the membrane potential of neuron i while $y_i(t)$, $z_i(t)$, and $x_i(t) = 1 - y_i(t) - z_i(t)$ represent the active, inactive, and available fraction of resources of the corresponding synapses. The potential $v_i(t)$ is reset to 0 at times $t_i(m)$ when it reaches the threshold $v_i[t_i(m)] = 1$. At $t_i(m)$, a spike activates a fraction u of the available resources, and the activation is modeled as a spike train $S_i(t) = \sum_m \delta[t - t_i(m)]$. Neurons are characterized by the coupling constant gk_i, randomly extracted from the distribution $P(k_i)$. Nk_i can be interpreted as the effective number of neural synapses interacting with neuron i, i.e., its in degree [44]. In this framework, k_i is the only relevant topological feature of the neural network and it justifies the DMF name. In a mean field description, the incoming synaptic current can be written as the average of the active resources $Y(t) = N^{-1} \sum_{i=1}^{N} y_i(t)$.

By introducing an event driven map [47], the DMF approach allows for very effective numerical simulations and it has been shown to reproduce the relevant collective dynamics for networks with large finite connectivity and metrical features [48] (see Supplemental Material [49]).

Equations (1)–(3) are characterized by three time scales: the period of the oscillating noninteracting neuron $T = \log[a/(a-1)]$, the recovery time τ_R, and the synaptic decay time τ_{in}. The regime $\tau_{\text{in}} \lesssim T$ has been studied in detail in Refs. [44,48,55,56], and it features a transition from a quasisynchronous to an asynchronous phase as a function of g and of the shape of $P(k_i)$. Here we will focus instead on the regime $\tau_{\text{in}} \ll T \ll \tau_R$, setting $a = 1.3$, $\tau_R = 10$ and varying τ_{in} between 10^{-1} and 10^{-5}. These parameters are consistent with those selected in Ref. [46], where they have been chosen on the basis of biological motivations.

Mean field.—The presence of a further nontrivial phase can be put into evidence by considering the simple in-degree distribution $P(k_i) = \delta(k_i - k_0)$. In this fully MF case, where all the coupling constants are equal, all neurons become completely synchronized after an initial transient state, as shown in the Supplemental Material [49]. Hence, Eqs. (1)–(3) reduce to the equations of a single neuron with coupling k_0 and $Y(t) = y(t)$. The dynamics can be rewritten as an event driven Poincaré map in z_n and y_n, representing the inactive and active resources before the nth synchronous spiking event (see Supplemental Material [49]),

$$y_{n+1} = e^{-(\Delta_n/\tau_{\text{in}})}[y_n + u(1 - y_n - z_n)], \qquad (4)$$

$$z_{n+1} = -e^{-(\Delta_n/\tau_{\text{in}})} \frac{y_n + u(1 - y_n - z_n)}{1 - \tau_{\text{in}}/\tau_R}$$
$$+ e^{-(\Delta_n/\tau_R)} \left(z_n + \frac{y_n + u(1 - y_n - z_n)}{1 - \tau_{\text{in}}/\tau_R} \right), \qquad (5)$$
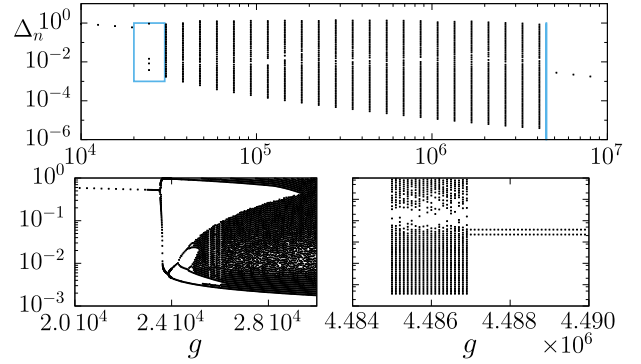

FIG. 1. Feigenbaum bifurcation diagram for the MF TUM model in Eqs. (4)–(5) with $\tau_{\text{in}} = 10^{-3}$. The attractor for the interspike interval of the network Δ_n is shown as a function of the coupling g. Upper panel: bifurcation diagram in the full relevant range of the parameter g. Lower-left panel: magnification on the period doubling cascade at the first transition. Lower-right panel: magnification on the second transition. The blue rectangles in the upper panel indicate the zooming regions of the lower panels.

where the time interval Δ_n between the nth and the $(n+1)$th spiking event is obtained from

$$1 = a - e^{-(\Delta_n/\tau_{\text{in}})} \frac{g\tau_{\text{in}}k_0[y_n + u(1 - y_n - z_n)]}{1 - \tau_{\text{in}}}$$
$$- e^{-\Delta_n} \left(a - \frac{g\tau_{\text{in}}k_0[y_n + u(1 - y_n - z_n)]}{1 - \tau_{\text{in}}} \right). \qquad (6)$$

When $\tau_{\text{in}} \ll T \ll \tau_R$, an insight on the dynamics can be achieved by considering the opposite regimes of weak and strong interaction, i.e., when $gk_0Y(t)$ or $a - v_{k_0}(t)$ are negligible in Eq. (1), respectively. In both extreme regimes, the map in Eqs. (4)–(6) can be solved, and it features a fixed point corresponding to a periodic solution in the continuous dynamics (see Supplemental Material [49] for details). In particular, in the weak coupling regime, the periodicity is trivially T, and the interaction term remains negligible if $gk_0\tau_{\text{in}} \ll \tau_R/T$. On the other hand, if the $a - v_{k_0}(t)$ term can be ignored, the system displays a much faster periodicity: $T_f = \tau_R/(gk_0\tau_{\text{in}})$ and the approximations hold only if $gk_0\tau_{\text{in}} \gg \tau_R/\tau_{\text{in}}$.

If $\tau_R/T \ll gk_0\tau_{\text{in}} \ll \tau_R/\tau_{\text{in}}$, neither the weak nor the strong coupling conditions are satisfied, and the competition between the terms with a slow and a fast dynamics plays a nontrivial role, destroying the presence of a periodic evolution. Such a behavior can be analyzed by means of the bifurcation diagram [57] of Δ_n as a function of g at fixed τ_{in}. Figure 1 shows the presence of a stable fixed point for small and large values of g, describing a slow and a fast periodic regime, respectively. For an intermediate value, a period doubling appears first; then, at $g > g'(\tau_{\text{in}})$, the distribution of Δ_n becomes continuous. The Δ_n becomes again delta-distributed for $g > g''(\tau_{\text{in}})$. In the Supplemental Material [49] we show that for $g'(\tau_{\text{in}}) < g < g''(\tau_{\text{in}})$ the
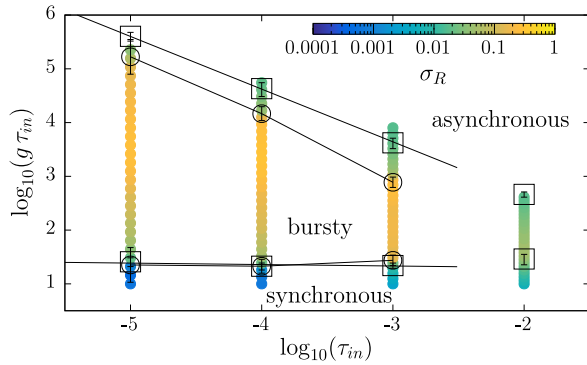
FIG. 2.   Dynamical phase diagram of the MF and DMF models in terms of the coupling constants g and of the synaptic time scale τ_{in}. MF model: The squares indicate the g values at which the transition to chaos (along with the discontinuity of the interspike time standard deviation) takes place (see Supplemental Material [49]). The black lines are linear fits. DMF model: Each colored point corresponds to a simulation, the color code indicating σ_R at the corresponding value of (g, τ_{in}). The intervals of g containing the discontinuity (cf. Fig. 3) are signaled with black circles.

FIG. 3.   Standard deviation of the Kuramoto parameter, σ_R versus g for the DMF model with $\tau_{\mathrm{in}} = 10^{-3}$ and five values of N. In the quasisynchronous and bursty phases the data corresponding to the two larger values of N overlap within their statistical errors, indicating convergence in size, while deep in the asynchronous phase they decrease as $\sim N^{-1/2}$. Inset: temporal average of $R(t)$, showing that the larger sizes have attained their asymptotic value in all the phases. The vertical stripes are common to all the figures in the article and indicate the apparent discontinuity of $\langle R \rangle$ for the largest sizes.

maximum Lyapunov exponent [58] becomes positive, a signature of the presence of chaos. In the fully MF system with N neurons, this is an example of synchronous chaos [42,43]. The phase diagram in Fig. 2 shows that the τ_{in} dependence of the boundaries of the chaotic phase (squares) is consistent with the continuous lines, obtained by the weak and strong coupling limit arguments. The critical values for g and τ_{in} depend on a, i.e., the intrinsic period of the neuron; the chaotic dynamics is observed at higher τ_{in} by considering smaller a (see Supplemental Material [49]). Taking the limit $\tau_{\mathrm{in}} \to 0$ with $g_{\mathrm{eff}} = gk_0\tau_{\mathrm{in}}$ constant in Eqs. (4)–(6), one obtains a single variable map as a function of g_{eff}, a and τ_R only, that can be studied analytically (see Supplemental Material [49]). This simpler map confirms the presence of a genuine chaotic dynamical phase.

Degree based mean field.—Let us now focus on the multisite DMF model with heterogeneous couplings extracted from the distribution $P(k_i)$. We consider a Gaussian $P(k_i)$ with average $\mu = 0.7$ and standard deviation $\sigma = 0.077$, although our results are robust for different distributions (see Supplemental Material [49] for a discussion). A relevant quantity describing the level of synchronization of the neurons is the Kuramoto parameter [59]: $R(t) = (1/N)|\sum_{i=1}^{N} e^{\iota\phi_i(t)}|$, where $\phi_i(t)$ is the phase of neuron i at time t:

$$\phi_i(t) = 2\pi \frac{t - t_i(m)}{t_i(m+1) - t_i(m)}, \qquad (7)$$

where $t_i(m)$ is the mth spike of neuron i and $t \in [t_i(m), t_i(m+1)]$. In Fig. 3, the time average $\langle R \rangle$ of the Kuramoto parameter and its fluctuations σ_R are displayed as a function of g. At small couplings, $\langle R \rangle \approx 1$ and
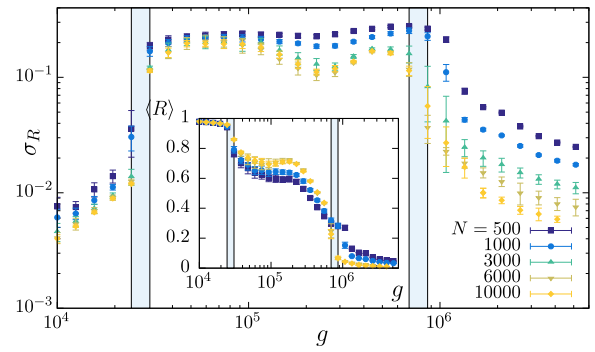
the fluctuations are small, as the systems is in a *quasisynchronous* phase. At large g, $\langle R \rangle$ becomes very small ($\langle R \rangle \to 0$ with increasing N), consistently with a periodic *asynchronous* phase. In the irregular, *bursty*, regime, $\langle R \rangle$ exhibits moderate values and, more significantly, its fluctuations grow abruptly by an order of magnitude; this is a signal of a complex dynamical phase, illustrated in the raster plot in the inset of Fig. 4 (each dot corresponds to a spike of neuron i at time t). The fluctuations of $\langle R \rangle$ originate from the alternations of synchronous events with asynchronous phases characterized by smaller bursts where only a subset of the neurons fires simultaneously. The main plot of Fig. 4 shows that the size s of such bursts, or avalanches, is broadly distributed (see Supplemental Material [49] for a detailed definition of burst size).
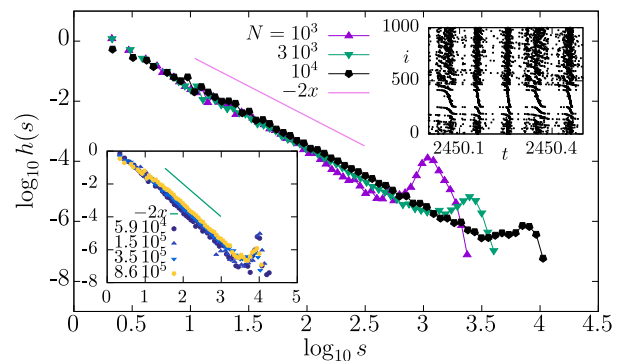

FIG. 4.   Avalanche size histogram $h(s)$ of the DMF model, $\tau_{\mathrm{in}} = 10^{-3}$ and $g = 3.5 \times 10^5$ in the bursty regime, for several values of N. Upper inset: a fragment of the raster plot for the same system. Lower inset: $\log_{10} h(s)$ for $N = 10^4$ and various values of g across the bursty phase.
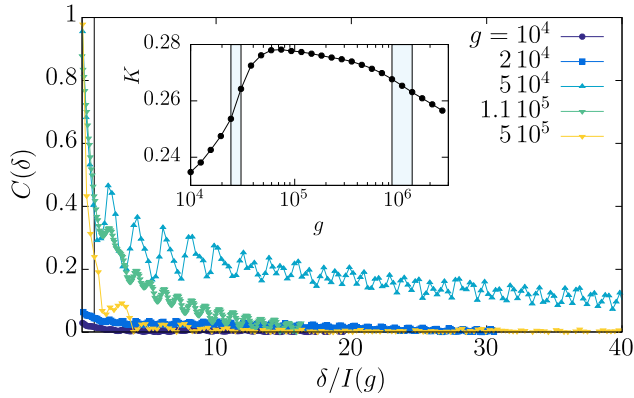
FIG. 5. Main plot: connected correlation function C as a function of the time difference δ in units of the average interspike time $I(g)$, for several values of g in the DMF model with $\tau_{in} = 10^{-3}$, $N = 800$. For values of g in the bursty phase, the correlation remains high even after large time differences. Inset: Kolmogorov complexity of the DMF model, $\tau_{in} = 10^{-3}$, $N = 10^3$, and the spike time differences Δ_n stored with 14 digits of precision.

Interestingly, the distribution is compatible with a power law $h(s) \sim s^{-\gamma}$ followed by a bump. The power γ, close to 2 (see Supplemental Material [49]), does not depend significantly on N, nor on g for a wide g range in the bursty phase. Finally, the peaks at large s in the distributions correspond to synchronous events where all neurons fire quasisimultaneously, and their position scales with the system size.

The natural issue is the relation between the chaotic phase in the single site MF model and the bursty-avalanche regime of the multisite DMF approach. In the Supplemental Material [49] we show that also the bursty phase is characterized by a chaotic dynamics with positive Lyapunov exponents. In Fig. 2 we have super-imposed the dynamical phase diagrams of the MF and DMF models. In the DMF, the transitions points (circles) are set at the g intervals at which the abrupt increments of the fluctuations of the Kuramoto parameter take place (cf. Fig. 3). In the MF case, the squares indicate the values of g at which the transitions to chaos occur. While the phase diagrams slightly differ, the phase diagram of the DMF model converges continuously to that of the MF model in the limit of vanishing width of the distribution $P(k_i)$, as illustrated in the Supplemental Material [49]. This scenario suggests that the bursty regime arises from the introduction of disorder on a system with synchronous chaos, so that neurons with different coupling k_i do not fire simultaneously and the synchronous solution loses stability.

In the DMF model, the transition to the bursty collective behavior also corresponds to the presence of large temporal correlations. We define the time dependent *complex correlation*, $c(\delta, t) = (1/N) \sum_{i=1}^{N} e^{\iota \phi_i(t)} e^{-\iota \phi_i(t+\delta)}$, where $\phi_i(t)$ is the Kuramoto phase (7), along with the *connected*

correlation function, $C(\delta) = |\langle c(\delta, t) \rangle_t| - |\langle c(\mathcal{T}, t) \rangle_t|$, as the temporal average $\langle \cdot \rangle_t$ of c over a sufficiently large interval of times t, minus its stationary value at a sufficiently large time difference, $\delta = \mathcal{T}$ (for details at this regard see the Supplemental Material [49] section). $C(\delta)$ measures in this way the average amount of correlation between spike configurations separated by a time delay δ. The quantity $C(\delta)$ (see Fig. 5, main panel) reveals the existence of large correlations for times δ much larger than the average interspike time, $I(g)$, only in the bursty regime (for $3 \times 10^4 \lesssim g \lesssim 10^5$ at $\tau_{in} = 10^{-3}$), while in the synchronous and asynchronous regimes, $C(\delta)$ decays faster to its asymptotic value.

Another interesting quantity in the temporal series of neural firing patterns is the amount of information they can sustain. In information theory, the Kolmogorov complexity (KC) of a data sequence determines the length of the minimum computer program generating it, hence being a measure of the sequence predictability [60]. KC has been related to the computational power of artificial neural networks [61], and used in the quantitative characterization of epileptic EEG recordings [62]. We consider the KC of the raster plot, interpreting it as an estimation of the amount of information that can be codified in the dynamical signal (see the details of the KC estimation in the Supplemental Material [49] section). The numerical results for the DMF model reveal that the KC as a function of g (see the inset of Fig. 5) presents a maximum in the bursty regime (around $g \simeq 6 \times 10^4$ for $\tau_{in} = 10^{-3}$).

In summary, we have reported the existence of a dynamical phase occurring in a network of purely excitatory LIF neurons connected with synaptic plasticity. This phase, identified by average statistical properties of the Kuramoto parameter, is strongly chaotic and it differs from previously known irregular phases for similar models, e.g., phases with chaotic transient dynamics [31,63]. The chaotic phase must also be distinguished from previous irregular regimes observed in spiking neural models, namely *weak* chaos in purely excitatory disordered networks [64] or *stable* chaos in inhibitory ones [65–67]. The emergent dynamical regime occurs in a large region of the phase diagram, and it is separated by two dynamical transitions from the quasisynchronous and asynchronous regimes. Chaos is preserved in the presence of disordered couplings. In that case, interestingly, the chaotic phase also features characteristic power law distributed avalanches. By properly defining temporal correlations and tools from information theory, we show that the additional bursty phase is strongly correlated and it carries a relevant amount of information compared to the quasisynchronous and the asynchronous phases.

[1] T. P. Vogels, K. Rajan, and L. Abbott, Annu. Rev. Neurosci. **28**, 357 (2005).

[2] E. Hulata, V. Volman, and E. Ben-Jacob, Nat. Comput. **4**, 363 (2005).

[3] Y. Shu, A. Hasenstaub, and D. A. McCormick, Nature (London) **423**, 288 (2003).

[4] X.-J. Wang, Physiol. Rev. **90**, 1195 (2010).

[5] A. Destexhe, S. W. Hughes, M. Rudolph, and V. Crunelli, Trends Neurosci. **30**, 334 (2007).

[6] J. Hesse and T. Gross, Front. Syst. Neurosci. **8** (2014).

[7] M. V. Sanchez-Vives and D. A. McCormick, Nat. Neurosci. **3**, 1027 (2000).

[8] L. F. Abbott and C. van Vreeswijk, Phys. Rev. E **48**, 1483 (1993).

[9] C. van Vreeswijk, Phys. Rev. E **54**, 5522 (1996).

[10] J. Kadmon and H. Sompolinsky, Phys. Rev. X **5**, 041030 (2015).

[11] N. Brunel, J. Comput. Neurosci. **8**, 183 (2000).

[12] C. Kirst, T. Geisel, and M. Timme, Phys. Rev. Lett. **102**, 068101 (2009).

[13] E. Montbrió, D. Pazó, and A. Roxin, Phys. Rev. X **5**, 021028 (2015).

[14] D. Hansel and G. Mato, Neural Comput. **15**, 1 (2003).

[15] S. Panzeri, R. S. Petersen, S. R. Schultz, M. Lebedev, and M. E. Diamond, Neuron **29**, 769 (2001).

[16] J. F. Mejias, H. J. Kappen, and J. J. Torres, PLoS One **5**, e13651 (2010).

[17] R. Livi, Chaos Solitons Fractals **55**, 60 (2013).

[18] B. D. Burns and A. C. Webb, Proc. R. Soc. B **194**, 211 (1976).

[19] M. London, A. Roth, L. Beeren, M. Hausser, and P. E. Latham, Nature (London) **466**, 123 (2010).

[20] J. M. Beggs and D. Plenz, J. Neurosci. **23**, 11167 (2003).

[21] R. Segev, Y. Shapira, M. Benveniste, and E. Ben-Jacob, Phys. Rev. E **64**, 011920 (2001).

[22] T. Petermann, T. C. Thiagarajan, M. A. Lebedev, M. A. Nicolelis, D. R. Chialvo, and D. Plenz, Proc. Natl. Acad. Sci. U.S.A. **106**, 15921 (2009).

[23] S. El Boustani, O. Marre, S. Béhuret, P. Baudot, P. Yger, T. Bal, A. Destexhe, and Y. Frégnac, PLoS Comput. Biol. **5**, e1000519 (2009).

[24] O. Kinouchi and M. Copelli, Nat. Phys. **2**, 348 (2006).

[25] S. Ostojic, Nat. Neurosci. **17**, 594 (2014).

[26] M. Monteforte and F. Wolf, Phys. Rev. X **2**, 041007 (2012).

[27] D. R. Chialvo, Nat. Phys. **6**, 744 (2010).

[28] P. Massobrio, L. de Arcangelis, V. Pasquale, H. J. Jensen, and D. Plenz, Front. Syst. Neurosci. **9**, 22 (2015).

[29] D. J. Amit and N. Brunel, Cereb. Cortex **7**, 237 (1997).

[30] C. van Vreeswijk and H. Sompolinsky, Science **274**, 1724 (1996).

[31] J. M. Cortes, M. Desroches, S. Rodrigues, R. Veltz, M. A. Muñoz, and T. J. Sejnowski, Proc. Natl. Acad. Sci. U.S.A. **110**, 16610 (2013).

[32] A. Levina, J. M. Herrmann, and T. Geisel, Nat. Phys. **3**, 857 (2007).

[33] J. A. Bonachela and M. A. Muñoz, J. Stat. Mech. (2009) P09009.

[34] J. A. Bonachela, S. de Franciscis, J. J. Torres, and M. A. Muñoz, J. Stat. Mech. (2010) P02015.

[35] D. Millman, S. Mihalas, A. Kirkwood, and E. Niebur, Nat. Phys. **6**, 801 (2010).

[36] V. Volman, I. Baruchi, E. Persi, and E. Ben-Jacob, Physica A (Amsterdam) **335**, 249 (2004).

[37] L. de Arcangelis, C. Perrone-Capano, and H. J. Herrmann, Phys. Rev. Lett. **96**, 028107 (2006).

[38] S. di Santo, R. Burioni, A. Vezzani, and M. A. Muñoz, Phys. Rev. Lett. **116**, 240601 (2016).

[39] F. Lombardi, H. J. Herrmann, C. Perrone-Capano, D. Plenz, and L. de Arcangelis, Phys. Rev. Lett. **108**, 228703 (2012).

[40] J. Touboul and A. Destexhe, PLoS One **5**, e8982 (2010).

[41] J. Touboul and A. Destexhe, Phys. Rev. E **95**, 012413 (2017).

[42] M. Ding and W. Yang, Phys. Rev. E **56**, 4009 (1997).

[43] J. F. Heagy, T. L. Carroll, and L. M. Pecora, Phys. Rev. E **50**, 1874 (1994).

[44] R. Burioni, M. Casartelli, M. di Volo, R. Livi, and A. Vezzani, Sci. Rep. **4**, 4336 (2014).

[45] E. M. Izhikevich, IEEE Trans. Neural Networks **15**, 1063 (2004).

[46] M. Tsodyks, A. Uziel, and H. Markram, J. Neurosci. **20**, RC50 (2000).

[47] R. Brette, Neural Comput. **19**, 2604 (2007).

[48] M. di Volo, R. Burioni, M. Casartelli, R. Livi, and A. Vezzani, Phys. Rev. E **90**, 022811 (2014).

[49] Supplemental Material at http://link.aps.org/supplemental/10.1103/PhysRevLett.118.098102 for details on analytical results and on numerical simulations, which includes Refs. [50–54].

[50] G. Benettin, L. Galgani, A. Giorgilli, and J. M. Strelcyn, Meccanica **15**, 9 (1980).

[51] I. Shimada and T. Nagashima, Prog. Theor. Phys. **61**, 1605 (1979).

[52] M. Tsodyks and H. Markram, Proc. Natl. Acad. Sci. U.S.A. **94**, 719 (1997).

[53] M. Tsodyks, K. Pawelzick, and H. Markram, Neural Comput. **10**, 821 (1998).

[54] A. Kaitchenko, Canadian Conference on Electrical and Computer Engineering 2004 (IEEE, New York, 2004), Vol. 4, p. 2255, http://ieeexplore.ieee.org/document/1347695/.

[55] M. di Volo, R. Livi, S. Luccioli, A. Politi, and A. Torcini, Phys. Rev. E **87**, 032801 (2013).

[56] R. Burioni, S. di Santo, M. di Volo, and A. Vezzani, Phys. Rev. E **90**, 042918 (2014).

[57] See e. g.: E. Ott, Chaos in Dynamical Systems (Cambridge University Press, Cambridge, England, 2001).

[58] G. Benettin, L. Galgani, A. Giorgilli, and J. M. Strelcyn, Meccanica **15**, 21 (1980).

[59] J. A. Acebrón, L. L. Bonilla, C. J. Pérez Vicente, F. Ritort, and R. Spigler, Rev. Mod. Phys. **77**, 137 (2005).

[60] M. Li and P. Vitányi, An Introduction to Kolmogorov Complexity and its Applications (Springer, New York, 1993).

[61] J. L. Balcazar, R. Gavalda, and H. T. Siegelmann, IEEE Trans. Inf. Theory **43**, 1175 (1997).

[62] A. Petrosian, in Proceedings of the Eighth IEEE Symposium on Computer-Based Medical Systems, Lubbock, Texas, 1995 (1995), p. 212.

[63] R. Zillmer, R. Livi, A. Politi, and A. Torcini, Phys. Rev. E **74**, 036203 (2006).

[64] S. Olmi, R. Livi, A. Politi, and A. Torcini, Phys. Rev. E **81**, 046119 (2010).

[65] R. Zillmer, N. Brunel, and D. Hansel, Phys. Rev. E **79**, 031909 (2009).

[66] E. Ullner and A. Politi, Phys. Rev. X **6**, 011015 (2016).

[67] D. Pazó and E. Montbrió, Phys. Rev. Lett. **116**, 238101 (2016).